Proceedings of the
American Control Conference
Baltimore, Maryland • June 1994

Design of an AutoLand Controller for a Carrier-Based F-14 Aircraft using $\mathcal{H}_\infty$ Output-Feedback Synthesis *

R. J. Niewoehner † Isaac I. Kaminer †

Abstract

The purpose of this paper is to present the results of a design effort to improve F-14 carrier landing performance by the incorporation of the Direct Lift Control into the aircraft's control system. This was done using a new design methodology whereby typical SISO design specifications were translated into the weighting functions of an $\mathcal{H}_\infty$ output-feedback synthesis problem. Finally, a technique is presented for the simplification of the structured uncertainty model for the air vehicles.

1 Introduction

Carrier approach and landing is a challenging multivariable control problem in which the aircraft states must all be carefully controlled in order to satisfy structural and safety-of-flight constraints. Automatic landing systems currently in service incorporate nested SISO controllers, which generally seek to regulate the angle-of-attack with the engines in the inner loop, while aerodynamic surfaces such as elevators or stabilators provide glideslope control. Since neither the engines nor the aerodynamic surfaces can control the altitude directly, their influence is indirect through a combination of other states. Direct Lift Control (DLC) provides the F-14 substantial authority to control altitude directly, but is dormant in the current system. Moreover, the DLC is driven by actuators whose bandwidth exceeds that of the other control surfaces. In this paper, a multivariable feedback controller is presented which seeks to exploit this powerful capability.

The design methodology presented here was developed to enable the control engineer to translate typical SISO design requirements into weighting functions for multivariable $\mathcal{H}_\infty$ synthesis. Moreover, once the SISO requirements have been satisfied, the $\mathcal{H}_\infty$ framework offers a natural way to expand the weighting functions to satisfy multivariable stability and performance robustness requirements.

In [1, 2, 3, 9] this technique was used to synthesize state-feedback controllers for aerospace and marine applications. In [8], where a controller for a flexible structure was designed, the methodology was extended to include an output feedback case. The methodology outlined here expands this previous work to include compliance with sensor bandwidth constraints.

Specifically, the methodology offers a simple and effective way to design feedback controllers satisfying specified:

- command-loop bandwidths,
- control-loop bandwidths,
- closed-loop damping,
- closed-loop sensor bandwidths.

It has been observed that an additional benefit of this methodology is that the resulting controllers do not cancel the undesirable modes of the open-loop plant. This is attributed to the weights chosen to satisfy the closed-loop damping requirement. The above objectives are pursued through a specific formulation of the synthesis model and systematic selection of the $\mathcal{H}_\infty$ synthesis weighting functions.

The appeal of this methodology is that the control designer is provided with a straightforward heuristic framework in which to implement $\mathcal{H}_\infty$ controllers without a detailed understanding of their theoretical basis. Moreover, the results of the design effort are assessed using familiar SISO figures-of-merit. The availability of good commercial software utilities, and ever-improving computational resources only enhance the viability of iterative design methods such as the one presented here. This methodology is suggested as one means of placing these tools into the hands of practicing control designers.

Lastly, a macroscopic method is proposed for accomodating structured model uncertainty in flight dynamics problems. The robustness of the resulting closed-loop system is then analyzed using established structured singlular value methods.

2 The Design and Analysis Tools

The principal design and analysis tools used for this effort included both the $\mathcal{H}_\infty$ synthesis and the μ-analysis functions of MATLAB's μ-Synthesis toolbox. These tools use a state-space representation of the linearized plant to determine a (sub)optimal $\mathcal{H}_\infty$ controller and to analyze the robustness of the closed-loop system. See [6] for specifics regarding the use of these tools, and additional references on their theoretical foundations. For the design procedure, the binary search threshold was set to approximately 5%. The $\mathcal{H}_\infty$ design tools pose the following constraint on the synthesis model, for all $s = j\omega$:

1. $\left[\begin{array}{c|c} sI - A & B_2 \\ \hline -C_1 & D_1 \end{array}\right]$ and D_1 must have full column rank, and
2. $\left[\begin{array}{c|c} sI - A & B_1 \\ \hline -C_2 & D_2 \end{array}\right]$ and D_2 must have full row rank.

3 Problem Statement

The objective of the controller design is to provide for precise automatic control of the approach and landing of a carrier-based aircraft in the vertical and longitudinal axes. In this section we describe both the plant to be controlled

*This work was supported in part by the Research Initiation Grant at the Naval Postgraduate School and Naval Air Systems Command under AIRTASK A546546TD

† Department of Aeronautics and Astronautics, Naval Postgraduate School, Monterey, CA 93943. Email: niewoehnerrj.nimitz@navair.navy.mil or kaminer@aa.nps.navy.mil

and the desired performance specifications. The notational convention uses uppercase letters to denote total values of the variables, while lower case letters denotes the perturbations of these variables around their nominal trim values.

3.1 Airplane and Model Description

The design problem to be solved here deals with the longitudinal motion of a fighter airplane and the control of the longitudinal rigid body dynamics. See [7] for a complete description of an airplane's equations of motion.

For the landing configuration, longitudinal control was provided by the engines, horizontal stabilators, and DLC. DLC was implemented by symmetric deflection of wing mounted spoilers. Sensors available included onboard accelerometers and gyros which provide pitch attitude, longitudinal acceleration, vertical acceleration, and pitch rate. The aircraft's air data system provided total airspeed, and angle of attack. Lastly, for automated approaches and landings, the altitude was determined by a shipboard tracking radar.

The model used for the design process was a linear model extracted from a nonlinear model built using aerodynamic coefficient data. This model was nonlinear in that while the aerodynamic derivatives were held constant, the equations of motion included the nonlinear influence of airspeed, gravity, as well as the dynamic coupling terms. The flight condition was a nominal approach point of 230 *fps*, at sea level, at a gross weight of 54,000 *lbs*. The linearized longitudinal model included five perturbation states: airspeed along body fixed x-axis (u), angle of attack (α), pitch rate (q), pitch attitude (θ) and altitude (h) and three control inputs: δ_{Stab}, δ_{Thrust} and δ_{DLC}. At this condition, the longitudinal rigid body motion was characterized by two second-order stable modes, the phugoid and short period, and an altitude integrator. The phugoid involved perturbations in u and h with nearly constant α with a natural frequency of 0.18 *rad/sec* and a damping ratio of 0.06. The short period mode involved perturbations in α and q, with constant u and h, at a natural frequency of 1.04 *rad/sec* and a damping ratio of 0.45. Control actuators were modeled by three first-order transfer functions with bandwidths of 20, 2.5 and 50 *rad/sec* for the stabilators, engine, and DLC, respectively. The complete system was consequently represented by an eighth order linear model.

3.2 Problem Description

The approach-to-landing problem could be fully characterized by several combinations of the variables in the state vector due to their mathematical and aerodynamic relationships. Likewise the control objectives could be achieved by tracking any one of these combinations. Systems in fleet use today incorporate nested SISO controllers, with the engine controlling angle of attack and the stabilators controlling either sink rate or flight path. Angle of attack was chosen as a control variable as it guaranteed a specified aerodynamic performance and touchdown attitude independent of gross weight. The remaining variables (such as airspeed and sink rate) were then dependent functions of the gross weight and the two controlled parameters. As deployed, the F-14's DLC was engaged for approach, such that the spoilers were deployed to their neutral DLC position. DLC was not utilized as part of the control system, however, and served only to increase both the drag and the trimmed power setting. Neither the engines nor the stabilators provided direct control over the flight path, but instead indirectly controlled the flight path through airspeed and pitch attitude. Performance may thereby have been sacrificed, as DLC was the only control effector which coupled directly into altitude, the most critical of the three parameters, and DLC actuator was the fastest of the three available actuators. Given three independent control effectors with sufficient control power, the F-14 had the resident capability to track three independent command signals. A multivariable approach to the control design permited inclusion of the DLC in the control system to improve performance. The control strategy chosen in this effort was to track altitude (h), and angle of attack (α), using stabilators, engines and DLC. The remaining degree of freedom was used to wash out the DLC in steady state.

3.3 Design Requirements

In light of the above, the controller was required to satisfy the following design requirements:

1. **Zero Steady State Error**

   - Achieve zero steady state values for all error variables in response to step commands in angle of attack, and ramp commands in altitude, while washing out DLC in steady state.

2. **Bandwidth Requirements**

   - The input-output command response bandwidth for all three command channels was to be approximately 1-2 rad/sec.
   - The control loop bandwidth was not to exceed 40 *rad/sec* for the DLC actuator, 20 *rad/sec* for symmetric stabilator, and 2 *rad/sec* for the engine. These numbers represented 80% of the corresponding actuator bandwidths to ensure that the actuators were not driven beyond their linear operating range.
   - The sensor response bandwidths were to be no more than 100 *rad/sec* for the gyros, accelerometers, and integrators, and no more than 5 *rad/sec* for the altitude, angle of attack and airspeed data.

3. **Closed Loop Damping**

   - The closed loop eigenvalues associated with physical states were to have the damping ratio of at least 0.6.

4. **Robustness**

   - No cancellation of lightly damped open-loop poles.
   - Simultaneous gain and phase margins of $\pm 6dB$ and 45 degrees in all control and sensor loops
   - Stability was to be guaranteed for simultaneous variations of 20% in the perturbed lift and drag forces and pitching moment.

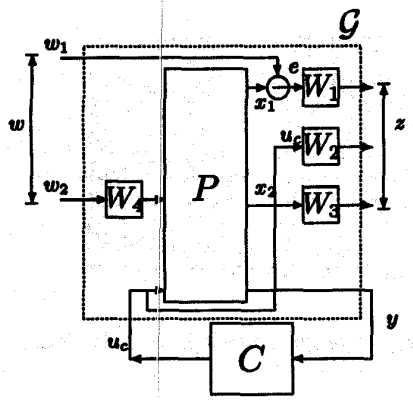

Figure 1: Synthesis Model

4 Controller Design

4.1 Synthesis Model

The synthesis model was the interface between the designer and the $\mathcal{H}_\infty$ controller synthesis algorithm. It's development is crucial to the design process.

Consider the feedback system in Fig 1. The synthesis model was developed from the linear model of the airplane by appending the depicted weights . The weights became the "knobs" which the designer adjusted to achieve the specified performance. Here C is the controller to be designed, P is the linear model of the F-14 and the block $\mathcal{G}$ within the dotted line is the synthesis model. The signal w_1 represents the commanded inputs which were to be tracked and was composed of:

$$w_1 = \begin{bmatrix} h_{cmd} & \alpha_{cmd} & DLC_{cmd} \end{bmatrix}'$$

The signal w_2 represents the noise inputs to each of the sensors, and disturbance inputs to the states of the plant. The signal u_c represents the control inputs to the system and is composed of the stabilator command, the thrust command, and the DLC command. The signals x_1 and x_2 were:

$$x_1 = \begin{bmatrix} h & \alpha & DLC \end{bmatrix}' \qquad x_2 = \begin{bmatrix} \dot{u} & \dot{\alpha} & \dot{q} & q & \dot{h} \end{bmatrix}'.$$

The signal e represents the tracking errors ($e = w_1 - x_1$).

The outputs of W_1, W_2 and W_3 together comprised the vector z. Since we required zero steady-state errors in tracking a ramp altitude command, and step speed and θ commands, the weighting function W_1 was initially chosen to be a diagonal matrix with terms: $(\frac{c_1}{s^2}, \frac{c_2}{s}, \frac{c_3}{s})$. W_1 was required to have full rank in order to satisfy detectability. W_2 and W_3 were constant diagonal matrices. W_2 was required have full rank in order to satisfy full column rank on D_2. Note that the elements of the vector x_2 are the rate terms on the principal states of the plant. Selection of x_2 is an important element of our methodology. Applying the weight W_3 to x_2, and including these signals in z, penalized activity in their corresponding states. The effect was the creation of rate feedback to augment damping, as with a classical controls approach. Importantly, W_3 did not need to have full rank. This permited us to set multiple weights to zero and use non-zero values only in the event that a particular signal was necessary to improve damping. The vector z was therefore comprised of the integrated errors, the control inputs, and the time derivatives of the principal states.

The signal y included the system's sensor outputs. Furthermore, y had to include the integral error state in order to satisfy the observability requirements of the design tools. Consequently, y was comprised of:

$$y = \begin{bmatrix} h & \alpha & v_t & \theta & n_z & n_x & q & \frac{h_e}{s^2} & \frac{\alpha}{s} & \frac{DLC}{s} \end{bmatrix}'.$$

4.2 The Design Procedure

The following steps outline the design procedure.

1. Set all W_3 weights to zero. Use state-feedback design to determine weights for W_1 and W_2, to satisfy the command and control-loop bandwidth requirements. Increasing W_1 weights increases the command bandwidths, while increasing W_2 weights decreases the broden-loop controller bandwidths.

2. If lightly damped closed-loop eigenvalues exist, determine participating states by eigenvector analysis. Adjust W_3 weights to include lightly damped states in output z. Increasing the weight in the corresponding W_3 entry had the effect of damping the dynamic activity of that state (analagous to classical rate feedback). Readjust W_1 and W_2 weights to maintain the previously achieved bandwidth specifications.

3. Given $W_{1,2,3}$ weights determined above, use measurement feedback design to determine the sensor noise weights in W_4 necessary to satisfy sensor response bandwidths. Increasing the weight in any channel of W_4 decreases the corresponding sensor bandwidth.

4. Determine the state process noise weights in W_4 by analysis of the broken-loop controller responses, adjusting the weights as necessary to approximate the cross-over frequencies observed for the state feedback design (This step is similar to Loop Transfer Recovery (LTR) technique for quadratic methods).

5. Readjust $W_{1,2,3}$ as required to maintain previously achieved specifications.

6. Evaluate resultant controller using linear and nonlinear simulation. Adjust weights if necessary.

7. Confirm satisfaction of other specification elements: robustness, damping, and no cancellation of lightly damped open-loop poles.

Steps 1 through 5 required 24 iterations and resulted in the determination of the following weights on z:
z =[$10\frac{h_e}{s^2}$, $30\frac{\alpha_s}{s}$, $5\frac{DLC_s}{s}$, $5\delta_{stab_{cmd}}$, $0.01\delta_{thrust_{cmd}}$, $\delta_{DLC_{cmd}}$, $10\dot{\alpha}$, $5\dot{q}$, $\dot{\theta}$]'. Note that three rate terms were required in order to augment the damping. The final ten sensor noise weights and three process noise weights were (W_4): 10^{-5}*[0.1 4 4 .01 .01 .01 0.1 10 10 1 5 5 5].

In step 6, the closed-loop linear system was simulated in order to determine whether reasonable actuator deflections were being used, and to ensure the desired tracking performance. The closed-loop system was initialized to level flight and then expected to intercept and track

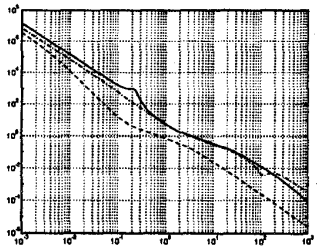

Figure 2: Broken-Loop Controller Responses

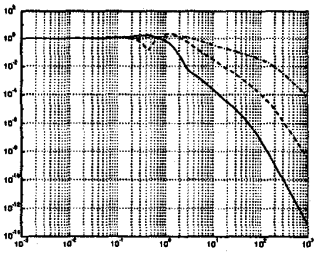

Figure 3: Closed-Loop Command Responses

an altitude ramp. While the altitude ramp was successfully intercepted and tracked, both α and DLC stabilized at values other than their set points. Examination of the transfer functions from altitude command to α and DLC revealed only a single zero at the origin within each numerator. In both cases there was an additional zero numerically close to zero, but insufficient to provide the desired washout characteristics. In order to provide the desired washout, an additional integrator was added to both channels in W_1. A new controller was then recalculated using this modified synthesis model with the same scalar weights determined above. Slight adjustment of the weights on z assisted the final determination of the bandwidths.

Figures 2, 3 and 4 depict the various bandwidths as satisfying their respective specifications, with the exception of the altitude command response which is slightly low at approximately 0.8 rad/sec. Examination of a Nyquist plot confirmed satisfaction of the gain and phase margin

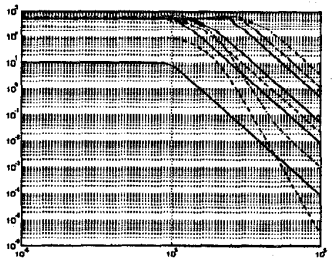

Figure 4: Sensor Responses

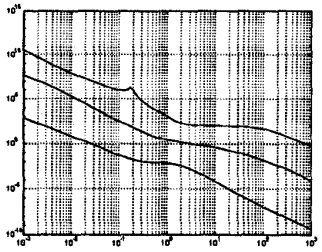

Figure 5: Control Loop Gain Singular Values

requirements. Eigen decomposition of the closed-loop system revealed a complex pair of eigenvalues which failed the damping ratio requirement (0.45). Examination of the corresponding eigenvector, however, revealed that no physical states and only controller states were significantly participating in this mode. Figure 5 depicts the singular values of the open-loop control responses. The presence of a clear spike at the frequency of the lightly damped phugoid mode and a small bump at the frequence of moderately damped short period mode indicates that the controller had not cancelled these open-loop poles. This was confirmed by analysis of the transmission zeros of the controller.

5 Robustness Analysis

5.1 Uncertainty Modeling

There are five terms which contribute to the nonlinear equations of motion: gravity, dynamic coupling, aerodynamic forces (states), thrust, and aerodynamic forces (controls). The first three terms are each state dependent. Additionally, since the aero forces are specified in stability axes, there is a state dependent rotational matrix required to convert them to the body axis system. Allowing x to represent the vector of the states ($[u, \alpha, q, \theta]$), and δ to represent the vector of the control effectors, these terms can be expressed as:

$$\begin{bmatrix} \dot{u} \\ \dot{\alpha} \\ \dot{q} \end{bmatrix} = \begin{matrix} F_{grav}(x) + F_{dyn}(x) + F_{thrust} + \\ R_{wb}(x)\left(F_{aero}(x) + F(\delta)\right) \end{matrix} \quad (1)$$

where $R_{wb}(x)$ is the wind to body axis rotation matrix.

We chose to model the uncertainty block, Δ, as a 3×3 diagonal matrix, where each δ_i represented a percentage of the nominal perturbation in the drag, lift and pitching moment due to aerodynamics. This was done to avoid the conservatism and errors implicit in using parametric uncertainty on each aerodynamic coefficient, when flight test is the origin of the stabilty derivative data.

Figure 6 depicts equation 1, with the force and moment contributions of the uncertainty block added directly prior to the state integrators. Note that since the uncertainty is expressed in stability axis coordinates, the input and output must be transformed to the body axis system. The signals w_δ and z_δ are the input and output of the closed-loop LFT $F_l(G, C)$ which must satisfy the structured small gain theorem.

Note that these signals could have been incorporated into w and z as a part of the synthesis model. An attribute of $\mathcal{H}_\infty$ control is that by including them, robustness could have been guaranteed *a priori* by explicitly

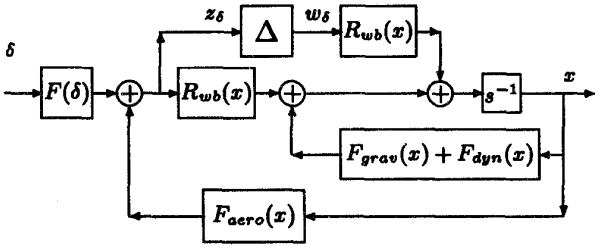

Figure 6: Uncertainty Model Connection

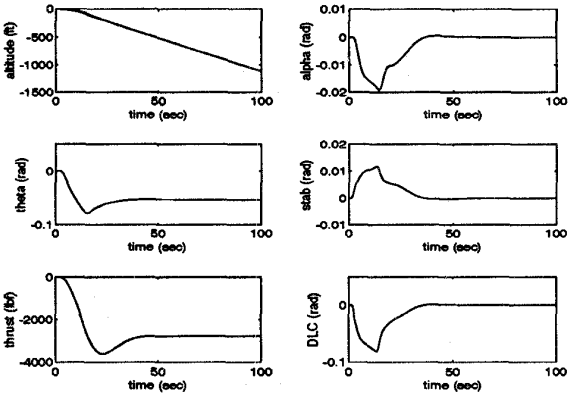

Figure 7: Nonlinear Simulation Results

enforcing the small gain theorem. Conservatively forcing robustness in this manner, however, may have compromised the ability of the designer to achieve the other desired performance specifications. Our approach was instead to proceed with the design using the synthesis model outlined above, without the uncertainty signals. When the other specifications had been attained, the robustness could be analysed, and if the robustness was satisfactory without the explicit inclusion of the uncertainty signals, no further effort would be required. In the event that the procedure failed to produce the specified level of robustness, then the uncertainty terms could have been appended to w and z and the procedure repeated using either pure $\mathcal{H}_\infty$ synthesis or D-K iteration.

5.2 μ Analysis

The supremum of the structured singular values for the closed loop systems were calculated to assess the robustness. In the case of the output-feedback controller, the singular values were determined from a direct linearization of the closed-loop nonlinear system, a portion of which is depicted in figure 6. Including the scaling by the desired robustness factor of 0.2, the output feedback controller had a norm of 0.42. A norm less than 1.0 indicates satisfaction of the structured small gain theorem and the robustness design specification by a factor slightly greater than two.

6 Nonlinear Simulation

With the design and mathematical analysis complete, as a final test, the controller was implemented on the original nonlinear model. The linear controller was implemented with the original nonlinear system using a $\mathcal{D}$-implementation (see [4]). As with the linear simulation performed above, the task was to intercept and track an altitude ramp, while appropriately controlling the other signals of interest. Results are depicted in figure 7, with values expressed as deviations from the trimmed level flight condition. Note that the DLC deflects briefly to establish the appropriate descent rate, and then washes out as the thrust stabilizes at the new trimmed condition. Likewise, α varies briefly during the tip over, and then returns to the desired trimmed α.

7 Conclusion

A measurement feedback controller was successfully designed to provide longitudinal control of an F-14 aircraft during automatic landing, and validated by nonlinear simulation. A key feature of the control was the exploitation of the aircraft's Direct Lift Control. Additionally, a methodology was detailed whereby SISO performance specifications were satisfied using the $\mathcal{H}_\infty$ synthesis method. Lastly, a method was presented for the macroscopic consideration of parametric uncertainties.

References

[1] I. Kaminer, P.P. Khargonekar, *Proc. of the 29th Conference on Decision and Control*, Honolulu, 1990, pp. 2981-2986.

[2] I. Kaminer, P. P. Khargonekar, and G. Robel, *IEEE Control Systems Magazine*, vol 10, pp. 13–21, 1990.

[3] I. Kaminer, A. M. Pascoal, C. Silvestre, and P. P. Khargonekar, *Proceedings of the 30th Conference on Decision and Control*, Dec. 1991, England, pp. 2350–2355.

[4] I. Kaminer, A. M. Pascoal, P. P. Khargonekar, and C. Thompson, *Proceedings of 1993 European Control Conference*, July 1993, pp. 787-791.

[5] P. P. Khargonekar, I. R. Petersen, and M. A. Rotea, *IEEE Transactions on Automatic Control*, vol. AC-33, no.8, pp.768-788, 1988.

[6] *μ-Analysis and Synthesis Toolbox: User's Guide*, Mathworks, 1991.

[7] J. Roskam, *Airplane Flight Dynamics and Automatic Flight Controls*, Roskam Aviation and Engineering Corporation, Lawrence, Kansas.

[8] N. Sivashankar, I. Kaminer, and P. P. Khargonekar, *Proceedings of the American Control Conference*, San Francisco, pp. 1612–1616, 1993.

[9] N. Sivashankar, I. Kaminer, and D. Kuechenmeister, preprint, September 1993.